










Adjustment of the PIF7-HFR1 transcriptional module activity controls plant shade adaptation

Sandi Paulišić¹ , Wenting Qin¹ , Harshul Arora Verasztó² , Christiane Then^{1†} , Benjamin Alary¹ , Fabien Nogue³ , Miltos Tsiantis⁴ , Michael Hothorn²  & Jaime F Martínez-García^{1,5,6,*} 

Abstract

Shade caused by the proximity of neighboring vegetation triggers a set of acclimation responses to either avoid or tolerate shade. Comparative analyses between the shade-avoider *Arabidopsis thaliana* and the shade-tolerant *Cardamine hirsuta* revealed a role for the atypical basic-helix-loop-helix LONG HYPOCOTYL IN FR 1 (HFR1) in maintaining the shade tolerance in *C. hirsuta*, inhibiting hypocotyl elongation in shade and constraining expression profile of shade-induced genes. We showed that *C. hirsuta* HFR1 protein is more stable than its *A. thaliana* counterpart, likely due to its lower binding affinity to CONSTITUTIVE PHOTOMORPHOGENIC 1 (COP1), contributing to enhance its biological activity. The enhanced HFR1 total activity is accompanied by an attenuated PHYTOCHROME INTERACTING FACTOR (PIF) activity in *C. hirsuta*. As a result, the PIF-HFR1 module is differently balanced, causing a reduced PIF activity and attenuating other PIF-mediated responses such as warm temperature-induced hypocotyl elongation (thermomorphogenesis) and dark-induced senescence. By this mechanism and that of the already-known of phytochrome A photoreceptor, plants might ensure to properly adapt and thrive in habitats with disparate light amounts.

Keywords *Cardamine hirsuta*; HFR1; PIFs; shade avoidance; shade tolerance

Subject Categories Evolution & Ecology; Plant Biology; Signal Transduction

DOI 10.15252/embj.2019104273 | Received 15 December 2019 | Revised 1

October 2020 | Accepted 16 October 2020 | Published online 2 December 2020

The EMBO Journal (2021) 40: e104273

Introduction

Acclimation of plants to adjust their development to the changing environment is of utmost importance. This acclimation relies on the plant's ability to perceive many cues such as water, nutrients, temperature, or light. Conditions in nature often involve

simultaneous changes in multiple light cues leading to an interplay of various photoreceptors to adjust plant growth appropriately (Pierik & Testerink, 2014; Mazza & Ballare, 2015; de Wit *et al.*, 2016; Ballare & Pierik, 2017; Fiorucci & Fankhauser, 2017). Nearby vegetation can impact both light quantity and quality. Under a canopy, light intensity is decreased and its quality is changed as the overtopping green leaves strongly absorb blue and red light (R) but reflect far-red light (FR). As a consequence, plants growing in forest understories receive less light of a much lower R to FR ratio (R:FR) than those growing in open spaces. In dense plant communities, FR reflected by neighboring plants also decreases R:FR but typically without changing light intensity. We refer to the first situation as canopy shade (very low R:FR) and the second as proximity shade (low R:FR). In general, two strategies have emerged to deal with shade: avoidance and tolerance (Valladares & Niinemets, 2008; Gommers *et al.*, 2013; Pierik & Testerink, 2014). Shade avoiders usually promote elongation of organs to outgrow the neighbors and avoid light shortages, reduce the levels of photosynthetic pigments to cope to light shortage, and accelerate flowering to ensure species survival (Casal, 2013). The set of responses to acclimate to shade is collectively known as the shade avoidance syndrome (SAS). In contrast, shade-tolerant species usually lack the promotion of elongation growth in response to shade and have developed a variety of traits to acclimate to low light conditions and optimize net carbon gain (Smith, 1982; Valladares & Niinemets, 2008).

In *Arabidopsis thaliana*, a shade-avoider plant, low R:FR is perceived by phytochromes. Among them, phyA has a negative role in elongation, particularly under canopy shade, whereas phyB inhibits elongation inactivating PHYTOCHROME INTERACTING FACTORS (PIFs), members of the basic-helix-loop-helix (bHLH) transcription factor family that promote elongation growth. In particular, PIFs induce hypocotyl elongation by initiating an expression cascade of genes involved in auxin biosynthesis and signaling [e.g., *YUCCA 8* (*YUC8*), *YUC9*, *INDOLE-3-ACETIC ACID INDUCIBLE 19* (*IAA19*), *IAA29*], and other processes related to cell elongation [e.g., *XYLOGLUCAN ENDOTRANSGLYCOSYLASE 7* (*XTR7*)]. Genetic

1 Centre for Research in Agricultural Genomics (CRAG), CSIC-IRTA-UAB-UB, Cerdanyola del Vallès, Campus UAB, Barcelona, Spain

2 Structural Plant Biology Laboratory, Section of Biology, Department of Botany and Plant Biology, University of Geneva, Geneva, Switzerland

3 Institut Jean-Pierre Bourgin, INRA, AgroParisTech, CNRS, Université Paris-Saclay, Versailles, France

4 Department of Comparative Development and Genetics, Max Planck Institute from Plant Breeding Research, Cologne, Germany

5 Institució Catalana de Recerca i Estudis Avançats (ICREA), Barcelona, Spain

6 Institute for Plant Molecular and Cellular Biology (IBMCP), CSIC-UPV, València, Spain

*Corresponding author. Tel: +34 963 878 627; E-mail: jaume.martinez@ibmcp.upv.es

[†]Present address: Department for Epidemiology and Pathogen Diagnostics, Julius Kühn-Institut, Federal Research Institute for Cultivated Plants, Braunschweig, Germany

analyses indicated that PIF7 is the key PIF regulator of the low R:FR-induced hypocotyl elongation with PIF4 and PIF5 having important contributions. Indeed, *pif7* mutant responds poorly to low R:FR compared to the *pif4 pif5* double or *pif1 pif3 pif4 pif5* quadruple (*pifq*) mutants, but the triple *pif4 pif5 pif7* mutant is almost unresponsive to low R:FR (Lorrain *et al*, 2008; Li *et al*, 2012; de Wit *et al*, 2016; van Gelderen *et al*, 2018). PhyB-mediated shade signaling involves other transcriptional regulators, such as *LONG HYPOCOTYL IN FR 1* (*HFR1*), *PHYTOCHROME RAPIDLY REGULATED 1* (*PAR1*), *BIM1*, *ATHB4*, or *BBX* factors, that either promote or inhibit shade-induced hypocotyl elongation (Sessa *et al*, 2005; Roig-Villanova *et al*, 2007; Sasidharan & Pierik, 2010; Cifuentes-Esquivel *et al*, 2013; Bou-Torrent *et al*, 2014; Gallemi *et al*, 2017; Yang & Li, 2017). *HFR1*, a member of the bHLH family, is structurally related to PIFs but lacks the phyB- and DNA-binding ability that PIFs possess (Galstyan *et al*, 2011; Hornitschek *et al*, 2012). *HFR1* inhibits PIF activity by heterodimerizing with them, as described for PIF1 (Shi *et al*, 2013), PIF3 (Fairchild *et al*, 2000), PIF4, and PIF5 (Hornitschek *et al*, 2009). Heterodimerization with *HFR1* prevents PIFs from binding to the DNA and altering gene expression. In this manner, *HFR1* acts as a transcriptional cofactor that modulates SAS responses, e.g., it inhibits hypocotyl elongation in seedlings in a PIF-dependent manner, forming the PIF-*HFR1* transcriptional regulatory module (Galstyan *et al*, 2011).

What mechanistic and regulatory adjustments in shade signaling are made between species to adapt to plant shade is a topic that has not received much attention until now. This question has been recently addressed performing comparative analyses between phylogenetically related species. In two related *Geranium* species that showed petioles with divergent elongation responses to shade, transcriptomic analysis led to propose that differences in expression of three factors, *FERONIA*, *THESEUS1*, and *KIDARI*, shown to activate SAS elongation responses in *A. thaliana*, might be part of the adjustments necessary to acquire a shade-avoiding or tolerant habit (Gommers *et al*, 2017). When comparing two related mustard species that showed divergent hypocotyl elongation response to shade, *A. thaliana* and *Cardamine hirsuta* (Hay *et al*, 2014), molecular and genetic analyses indicated that phyA, and to a lesser extent phyB, contributed to establish this divergent response. In particular, the identification and characterization of the *C. hirsuta* phyA-deficient *slender in shade 1* (*sis1*) mutant indicated that differential features of this photoreceptor in *A. thaliana* and *C. hirsuta* could explain their differential response to shade. Thus, stronger phyA activity in *C. hirsuta* wild-type plants resulted in a suppressed hypocotyl elongation response when exposed to low or very low R:FR (Molina-Contreras *et al*, 2019). These approaches indicated that the implementation of shade avoidance and shade tolerance involved the participation of shared genetic components. They also suggest that other responses co-regulated by these shared components will be accordingly affected.

With this frame of reference, we asked whether the phyB-dependent PIF-*HFR1* module was also relevant to shape the shade response habits in different plant species. We found that *C. hirsuta* plants deficient in *ChHFR1* gained a capacity to elongate in response to shade. We also report that *AtHFR1* and *ChHFR1* are expressed at different levels and encode proteins with different protein stability, caused by their different binding affinities with CONSTITUTIVE PHOTOMORPHOGENIC 1 (*COP1*), known to affect *AtHFR1* stability

under shade (Pacin *et al*, 2016). We propose that adaptation to plant shade in *A. thaliana* and *C. hirsuta* relies on the PIF-*HFR1* regulatory module. As PIFs regulate several other processes, we hypothesized that a set of responses co-regulated by the PIF-*HFR1* module are also affected and associated with the shade-avoidance and shade-tolerant habits. After exploring this possibility, we found that thermoregulation of hypocotyl elongation and dark-induced senescence, two well-known PIF-regulated responses (Koini *et al*, 2009; Stavang *et al*, 2009; Sakuraba *et al*, 2014), is consistently affected in *C. hirsuta*.

Results

HFR1 is required for the shade tolerance habit of *Cardamine hirsuta*

First, we wanted to determine if *HFR1* has a role in the shade-tolerance habit of *C. hirsuta*, i.e., whether *ChHFR1* contributes to inhibit hypocotyl elongation when this species is exposed to shade. For this purpose, we generated several *C. hirsuta* RNAi lines to downregulate *HFR1* expression (RNAi-*HFR1* lines). As expected, *ChHFR1* expression was attenuated in seedlings of two RNAi-*HFR1* selected lines (#01 and #21) compared to the wild type (*Ch*^{WT}) (Fig EV1A). When growing under white light (W) of high R:FR (> 1.5), hypocotyl length of these two RNAi-*HFR1* lines was undistinguishable from *Ch*^{WT} (Fig 1A). By contrast, under W supplemented with increasing amounts of FR (W + FR) resulting in moderate (0.09), low (0.05–0.06), and very low (0.02) R:FR (that simulated proximity and canopy shade) (Martinez-Garcia *et al*, 2014), the hypocotyl elongation of RNAi-*HFR1* seedlings was significantly promoted compared to *Ch*^{WT}, which was unresponsive (Fig 1A).

Using CRISPR-Cas9, we obtained two mutant lines of *ChHFR1* (named *chfr1-1* and *chfr1-2*) with a single nucleotide insertion in their sequence leading to a premature stop codon (Fig EV1C). These mutants showed a non-significant decrease of *ChHFR1* expression in W-grown seedlings (Fig EV1B). Similar to the RNAi-*HFR1* lines, their hypocotyls were undistinguishable from *Ch*^{WT} under W but elongated strongly in response to W + FR exposure (Fig 1B), showing a *slender in shade* (*sis*) phenotype. Together, we concluded that *HFR1* represses hypocotyl elongation in response to shade in *C. hirsuta*.

Exposure of *A. thaliana* wild-type (*At*^{WT}) and *Ch*^{WT} seedlings to low R:FR induces a rapid increase in the expression of various direct target genes of PIFs, including *PIF3-LIKE 1* (*PIL1*), *YUC8*, and *XTR7* (Fig 1C and D) (Ciolfi *et al*, 2013; Hersch *et al*, 2014; Molina-Contreras *et al*, 2019). The shade-induced expression of these genes was significantly higher in RNAi-*HFR1* and *chfr1* mutant lines compared to *Ch*^{WT} (Fig 1C and D), indicating that *ChHFR1* might repress shade-triggered hypocotyl elongation in part by downregulating the rapid shade-induced expression of these genes in *C. hirsuta*, as it was observed with *AtHFR1* in *A. thaliana* seedlings (Hornitschek *et al*, 2009).

HFR1 expression is higher in *Cardamine hirsuta* than in *Arabidopsis thaliana* seedlings

To test if the lack of elongation of *Ch*^{WT} hypocotyls in response to shade was caused by higher levels of *ChHFR1* expression in this

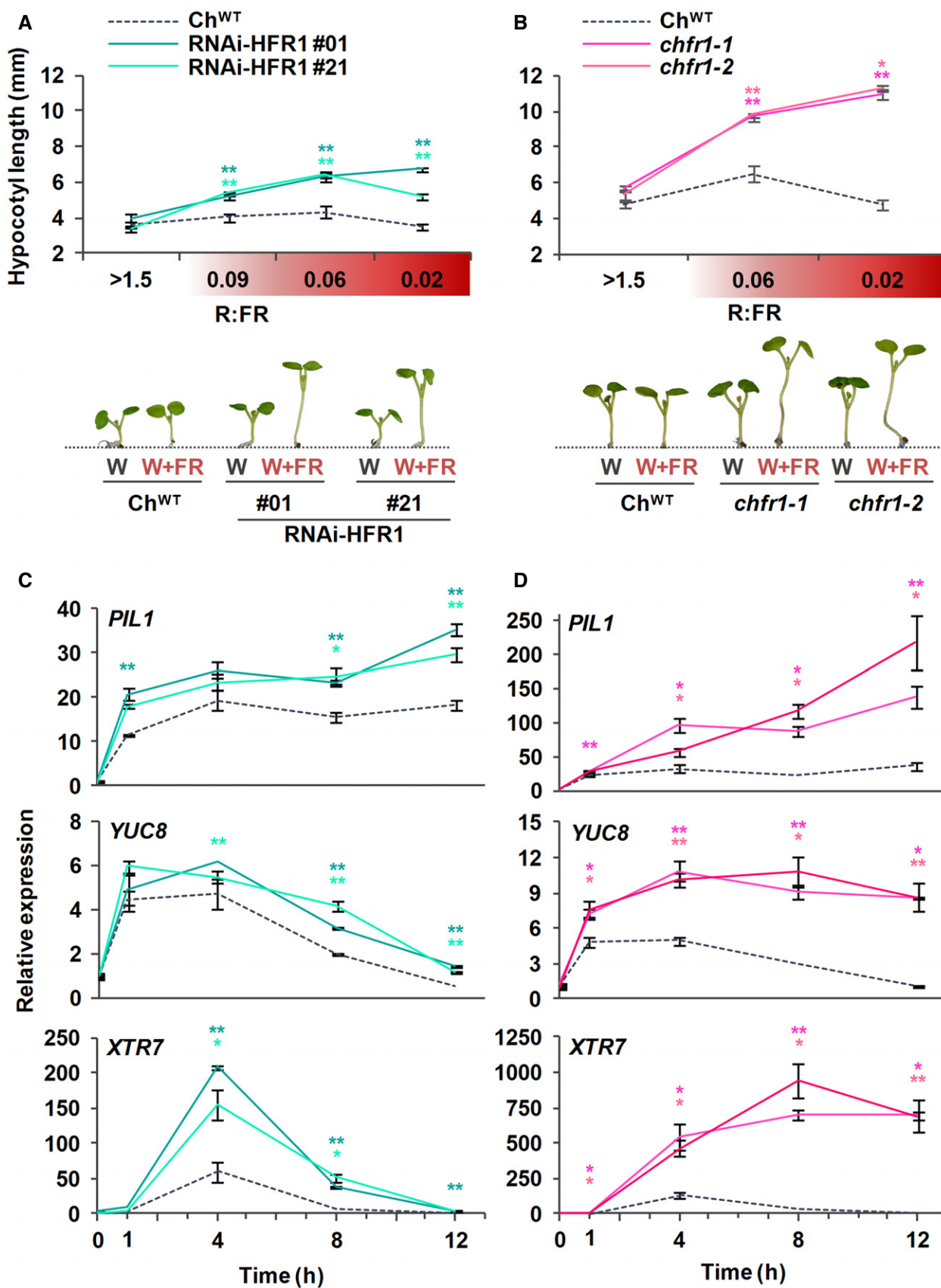


Figure 1.

Figure 1. Hypocotyls of *Cardamine hirsuta* seedlings with reduced levels of *ChHFR1* strongly elongate in response to simulated shade.

A, B Hypocotyl length of *Ch*^{WT}, (A) RNAi-*ChHFR1* transgenic, and (B) *chfr1* mutant seedlings grown under different R:FR. Seedlings were grown for 7 days in continuous W (R:FR > 1.5) or for 3 days in W then transferred to W supplemented with increasing amounts of FR (W + FR) for 4 more days, producing various R:FR. Aspect of representative 7-day-old *Ch*^{WT}, RNAi-HFR1 and *chfr1-1* seedlings grown in W or W + FR (R:FR, 0.02), as indicated, is shown in lower panel.

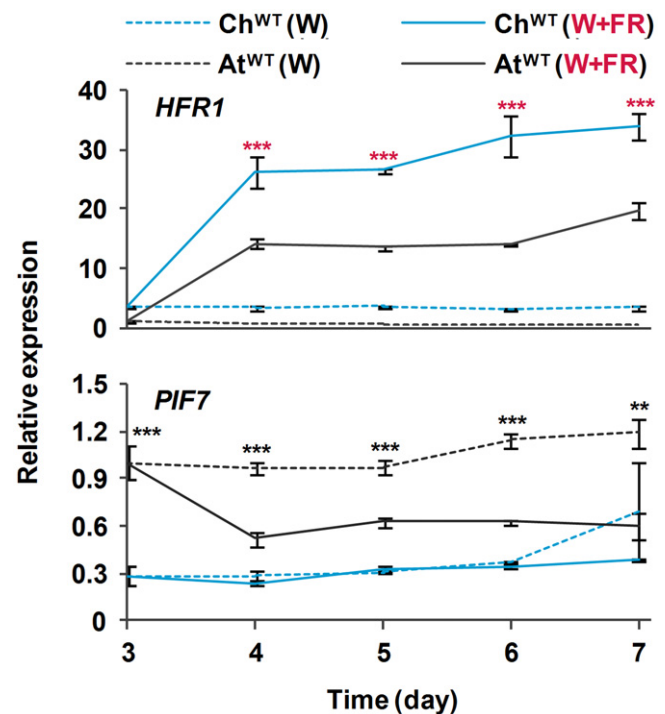
C, D Effect of W + FR exposure on the expression of *PIL1*, *YUC8*, and *XTR7* genes in seedlings of *Ch*^{WT}, (C) RNAi-HFR1, and (D) *chfr1* mutant lines. Expression was analyzed in 7-day-old W-grown seedlings transferred to W + FR (R:FR, 0.02) for 0, 1, 4, 8, and 12 h. Transcript abundance is normalized to *EF1α* levels.

Data information: Values are the means ± SE of three independent biological replicates relative to *Ch*^{WT} value at 0 h. Asterisks mark significant differences (Student's t-test: ***P*-value < 0.01; **P*-value < 0.05) relative to *Ch*^{WT} value at the same time point.

species, we used primer pairs that amplify *HFR1* (Fig EV2A) and three housekeeping genes (*EF1α*, *SPC25*, *YLS8*) in both species (Molina-Contreras *et al.*, 2019). As expected, expression of *HFR1* was induced in shade-treated seedlings of both species, in agreement with the presence of canonical PIF-binding sites (G-box, CACGTG) in the *HFR1* promoters (Martinez-Garcia *et al.*, 2000; Hornitschek *et al.*, 2009; Fig EV3A). More importantly, *ChHFR1* transcript levels were always higher than those of *AtHFR1* during the whole period analyzed (from days 3 to 7) (Fig 2). Because *HFR1* is part of the PIF-HFR1 regulatory module, we next compared transcript levels of *PIF* genes in both species. *PIF7* expression was significantly lower in *C. hirsuta* than in *A. thaliana* in either W or W + FR during the period analyzed (Fig 2). By contrast, *PIF4* expression was higher in *C. hirsuta* than in *A. thaliana*, whereas that of *PIF5* was similar in both species (Fig EV2B). Together, these results indicated that whereas *HFR1* expression is enhanced, that of *PIF7* is globally attenuated in *Ch*^{WT} compared to *At*^{WT} seedlings. As a consequence, the PIF-HFR1 transcriptional module might be differently balanced in these species, with *HFR1* imposing a stronger suppression on the *PIF7*-driven hypocotyl elongation in the shade-tolerant *C. hirsuta* seedlings.

ChHFR1 protein is more stable than AtHFR1

A higher specific activity of *ChHFR1* compared to its orthologue *AtHFR1* might also contribute to the role of this transcriptional cofactor in maintaining the shade tolerance habit of *C. hirsuta*. To test this possibility, we transformed *A. thaliana hfr1-5* plants with constructs to express either *AtHFR1* or *ChHFR1* fused to the 3x hemagglutinin tag (3xHA). These genes were expressed under the transcriptional control of the 2 kb of the *AtHFR1* promoter (*pAt*), generating *hfr1>pAt:ChHFR1* and *hfr1>pAt:AtHFR1* lines (Fig 3A). Fusion of *pAt* to the *GUS* reporter gene resulted in *GUS* activity in cotyledons and roots of transgenic lines, with increased levels in hypocotyls of seedlings exposed for 2–4 h to W + FR (Fig EV3B). Several independent transgenic lines of each construct were analyzed for hypocotyl length (Appendix Fig S1), *HFR1* transcript levels and 3xHA-tagged protein abundance. In these lines, *HFR1* biological activity was estimated as the difference in hypocotyl length of seedlings grown under W + FR (Hyp_{W+FR}) and W (Hyp_W) (Hyp_{W+FR}-Hyp_W) (Molina-Contreras *et al.*, 2019). The potential to suppress the hypocotyl elongation in shade below that of *hfr1-5* seedlings would depend on the transcript level of *HFR1* and/or its protein levels. The *hfr1>pAt:ChHFR1* lines had shorter hypocotyls in shade (i.e., stronger global *HFR1* activity) compared to *hfr1>pAt:AtHFR1* lines of similar *HFR1* expression levels (Figs 3B and C, and EV3C), suggesting that total *HFR1* activity was higher in *hfr1>pAt:ChHFR1* than in *hfr1>pAt:AtHFR1* lines. However, we observed

**Figure 2. Levels of *HFR1* transcript are higher in *Cardamine hirsuta* than *Arabidopsis thaliana* seedlings.**

Seedlings of *Ch*^{WT} and *At*^{WT} were grown for 3 days in W then either kept under the same conditions or transferred to W + FR (R:FR, 0.02) for the indicated times. Plant material was harvested every 24 h. Transcript abundance of *HFR1* and *PIF7* was normalized to three reference genes (*EF1α*, *SPC25*, and *YLS8*). Expression values are the means ± SE of three independent biological replicates relative to the data of *At*^{WT} grown in continuous W at day 3. Asterisks mark significant differences (2-way ANOVA: ***P*-value < 0.01, ****P*-value < 0.001) between *Ch*^{WT} and *At*^{WT} when grown under W (black asterisks) or W + FR (red asterisks).

much higher abundance of *HFR1*-3xHA protein after shade exposure in *hfr1>pAt:ChHFR1* lines than in *hfr1>pAt:AtHFR1* lines with comparable levels of *HFR1* expression (Fig 3D), suggesting that the *ChHFR1* protein might be much more stable. Together, these results point to differences in protein stability (rather than in specific activity) as the main cause for the enhanced *HFR1* total activity of *ChHFR1* compared to *AtHFR1* in complemented lines.

AtHFR1 stability is affected by light conditions. In etiolated seedlings, exposure to W promotes stabilization and accumulation of *AtHFR1*, whereas in W-grown seedlings, high intensity of W increases its abundance (Duek *et al.*, 2004; Yang *et al.*, 2005). Importantly, *AtHFR1* stability has a strong impact on its biological activity

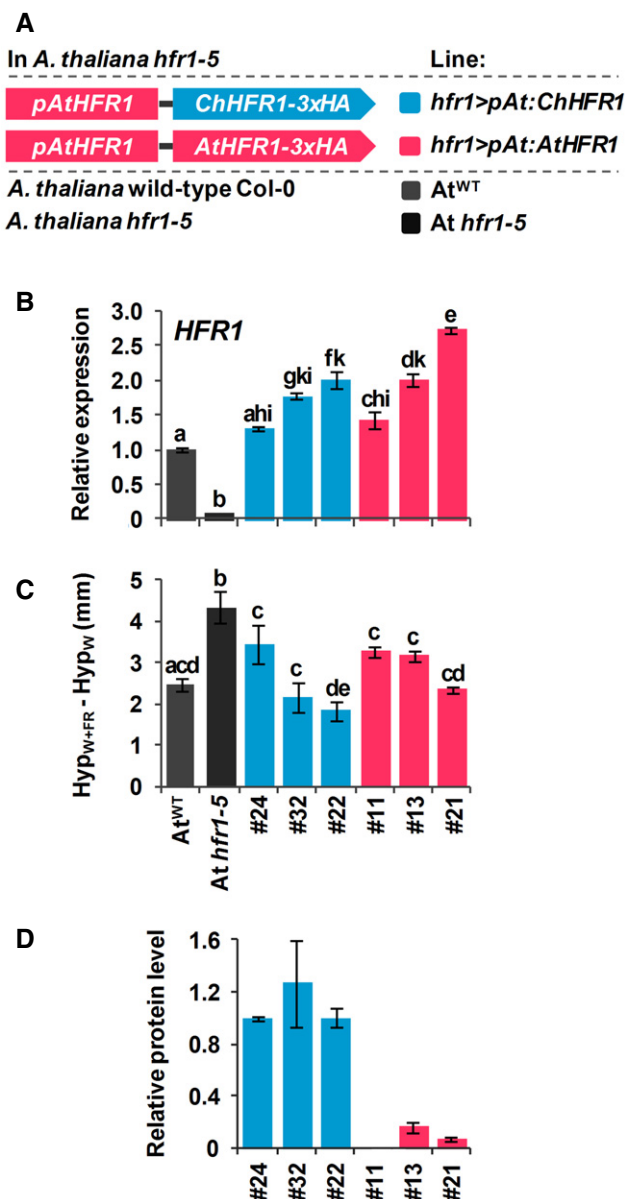


Figure 3. The activity of ChHFR1 is higher than that of AtHFR1 in *Arabidopsis thaliana* seedlings.

- A** Cartoon of constructs containing ChHFR1 or AtHFR1 under the HFR1 promoter of *Arabidopsis thaliana* (*pAtHFR1*) used to complement *hfr1-5* mutant of *A. thaliana* (*At hfr1-5*).
- B** Relative expression of HFR1 in seedlings of *At^{WT}*, *At hfr1-5*, *hfr1>pAt:ChHFR1* (in blue), and *hfr1>pAt:AtHFR1* (in red) lines grown under W + FR (R:FR, 0.02). Expression values are the means \pm SE of three independent biological replicates relative to the data of 7 days old *At^{WT}*. Transcript abundance is normalized to *UBQ10* levels.
- C** Elongation response of seedlings of the indicated lines grown for 7 days in continuous W or 2 days in W then transferred for 5 days to W + FR (R:FR, 0.02). The mean hypocotyl length in W (Hyp_W) and W + FR (Hyp_{W+FR}) of at least four biological replicates was used to calculate Hyp_{W+FR} - Hyp_W. Error bars represent SE.
- D** Relative HFR1 protein levels in seedlings of the indicated lines, normalized to actin protein levels, are the means \pm SE of three independent biological replicates relative to *hfr1>pAt:ChHFR1* line #22 that is taken as 1. Seedlings were grown for 7 days in continuous W ($\sim 20 \mu\text{mol}/\text{m}^2\cdot\text{s}^{-1}$) after which they were incubated for 3 h in high W ($\sim 100 \mu\text{mol}/\text{m}^2\cdot\text{s}^{-1}$) and transferred to W + FR (R:FR, 0.06) for 3 h.

Data information: Different letters denote significant differences (one-way ANOVA with the Tukey test, P -value < 0.05) among means. Source data are available online for this figure.

intensity in all our subsequent experiments to analyze ChHFR1 levels.

Next, we exposed *hfr1>pAt:ChHFR1* (line #22) and *hfr1>pAt:AtHFR1* (line #13) seedlings to W + FR (Fig 4A). Although HFR1 expression in both lines was similarly induced after 3 h of W + FR, *hfr1>pAt:ChHFR1* line displayed higher levels of recombinant HFR1 protein compared to *hfr1>pAt:AtHFR1* line after 3–6 h of W + FR exposure (Fig 4A), suggesting a higher stability of the *C. hirsuta* protein compared to the *A. thaliana* orthologue. ChHFR1 protein is more abundant than AtHFR1 also when transiently expressed to comparable levels in *Nicotiana benthamiana* (tobacco) leaves (Fig 4B and C). This indicates that the higher abundance of ChHFR1 is an intrinsic property of the protein that resides in its primary structure.

AtHFR1 is known to be targeted for degradation via the 26S proteasome in dark-grown seedlings. Shade also promotes AtHFR1 degradation compared to non-shade treatments (Pacin *et al*, 2016). Hence, ChHFR1 abundance might be similarly targeted, and the increased ChHFR1 protein stability might be due to differences in degradation kinetics, likely by the 26S proteasome. We addressed this possibility by treating tobacco leaf disks overexpressing ChHFR1 and AtHFR1 with the protein synthesis inhibitor cycloheximide (CHX) combined with shade (Fig 4D). This treatment resulted in a decrease in ChHFR1 and AtHFR1 protein levels. However, ChHFR1 degradation was significantly slower than that of AtHFR1 (Fig 4D), supporting that changes in degradation kinetics likely contribute to the observed differences in stability between ChHFR1 and AtHFR1.

Light- and shade-regulated degradation of AtHFR1 requires binding to COP1 and the COP1 E3 ubiquitin ligase activity. Binding to COP1 results in HFR1 ubiquitination, which targets HFR1 for degradation via the 26S proteasome (Jang *et al*, 2005; Yang *et al*, 2005; Pacin *et al*, 2016). COP1-interacting proteins harbor sequence-divergent Val-Pro (VP) motifs that bind the COP1 WD40 domain with different affinities (Lau *et al*, 2019).

as overexpression of stable forms of this protein leads to phenotypes resulting from enhanced HFR1 activity (Yang *et al*, 2005; Galstyan *et al*, 2011). As AtHFR1 and ChHFR1 primary structures are globally similar (Fig EV4A), we aimed to test if ChHFR1 stability is also light-dependent. We first examined ChHFR1 protein accumulation in response to different W intensities in seedlings of an *A. thaliana* *hfr1-5* line that constitutively express ChHFR1 (*hfr1>35S:ChHFR1*) (Fig EV4B). When grown in our normal W conditions ($\sim 20 \mu\text{mol}/\text{m}^2\cdot\text{s}^{-1}$), these seedlings accumulated low but detectable levels of ChHFR1; when transferred to higher W intensity ($\sim 100 \mu\text{mol}/\text{m}^2\cdot\text{s}^{-1}$), ChHFR1 levels increased 10-fold (Fig EV4C). As ChHFR1 is expressed under the constitutive 35S promoter, these results indicate that ChHFR1 protein accumulation is induced by high W intensity, as it has been described for AtHFR1 (Yang *et al*, 2005). This prompted us to pretreat W-grown seedlings with 3 h of high W

Inspection of the COP1 WD40–AtHFR1 complex structure (Lau *et al*, 2019) revealed that sequence differences between AtHFR1 and ChHFR1 map to the N-terminus of the VP peptide involved in the interaction with COP1 (Fig 5A). We hypothesized that

these sequence variations between HFR1 species may result in different COP1 binding affinities, affecting targeting and subsequent degradation of the two HFR1 orthologues. We thus quantified the interaction of synthetic AtHFR1 and ChHFR1 VP

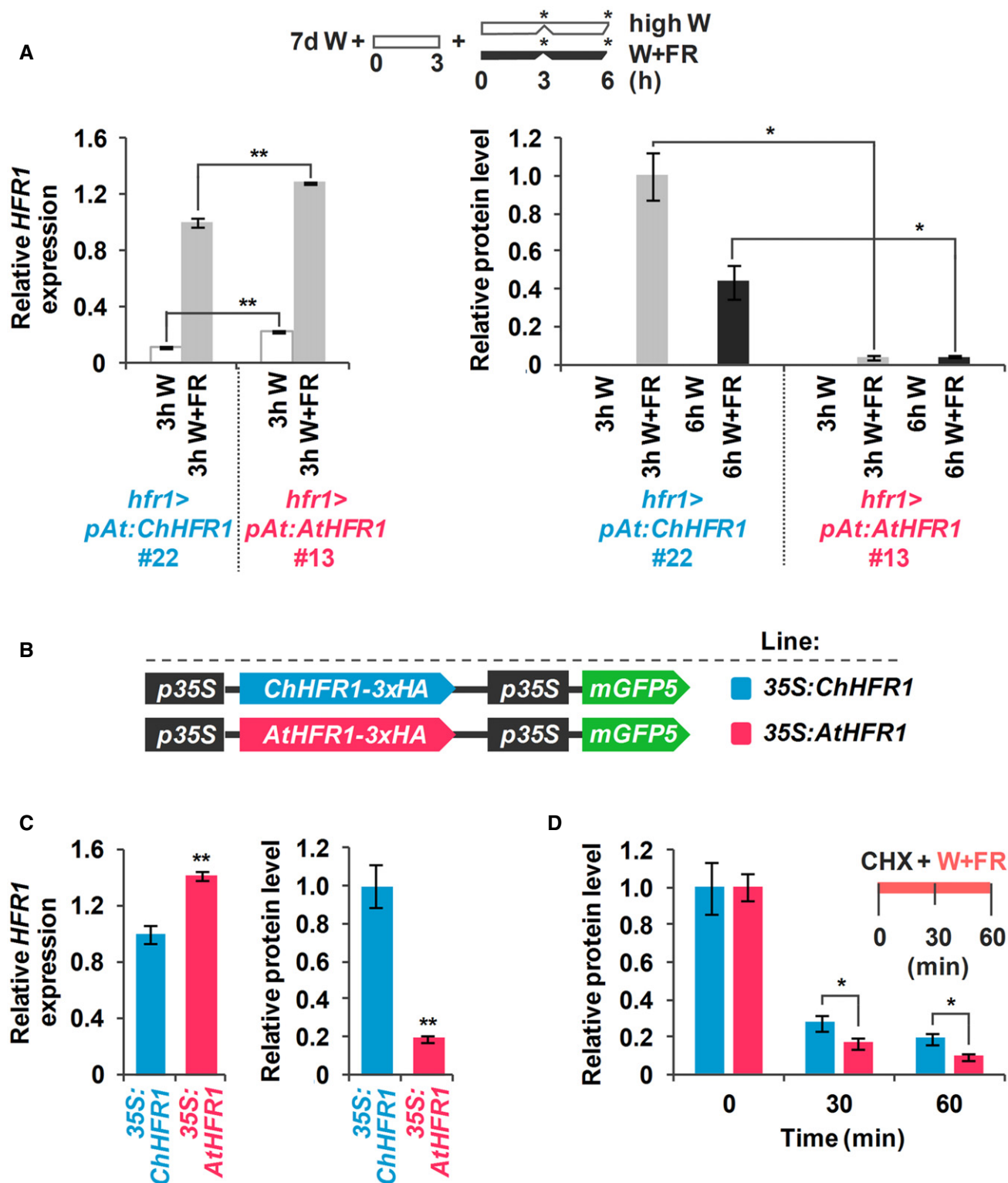


Figure 4.

Figure 4. ChHFR1 and AtHFR1 proteins show different stability in shade.

- A Expression of *HFR1* and protein levels of HFR1-3xHA in seedlings of *hfr1>pAt:ChHFR1* (line #22) and *hfr1>pAt:AtHFR1* (line #13). Seedlings were grown for 7 days in continuous W ($\sim 20 \mu\text{mol}/\text{m}^2\cdot\text{s}^2$) after which they were incubated for 3 h in high W ($\sim 100 \mu\text{mol}/\text{m}^2\cdot\text{s}^2$) and then either kept at high W or transferred to W + FR (R:FR, 0.06) for 3 or 6 h, as indicated in the cartoon at the top. Relative *HFR1* transcript levels, normalized to *UBQ10*, are the means \pm SE of three independent biological replicates relative to *hfr1>pAt:ChHFR1* #22 grown for 3 h under W + FR. Relative protein levels, normalized to actin, are the means \pm SE of three independent biological replicates relative to *hfr1>pAt:ChHFR1* #22. Samples were collected at data points marked in the cartoon with asterisks.
- B Cartoon of constructs containing *ChHFR1* or *AtHFR1* under the 35S promoter used for transient expression of transgenes in *N. benthamiana* leaves.
- C Relative *HFR1* transcript levels transiently expressed in tobacco leaves, normalized to the *GFP*, are the means \pm SE of three independent biological replicates (left). Relative HFR1 protein levels, normalized to the GFP levels, are the means \pm SE of four independent biological replicates (right). In (A) and (C), asterisks mark significant differences (Student's *t*-test: **P*-value < 0.05, ***P*-value < 0.01) between the indicated pairs.
- D Degradation of ChHFR1 (35S:ChHFR1) and AtHFR1 (35S:AtHFR1) in tobacco leaf disks treated with cycloheximide (CHX, 100 μM) for the indicated times. Tobacco plants were kept under high W ($\sim 200 \mu\text{mol}/\text{m}^2\cdot\text{s}^2$) for 3 days after agroinfiltration and then leaf circles were treated with W + FR (R:FR, 0.2) and CHX. Relative HFR1 protein levels (ChHFR1, blue bars; AtHFR1, red bars), normalized to the GFP levels, are the means \pm SE of four biological replicates relative to data point 0, taken as 1 for each line. Asterisks mark significant differences (2-way ANOVA: **P*-value < 0.05) between ChHFR1 and AtHFR1 at the same time point.

Source data are available online for this figure.

peptides with COP1 using microscale thermophoresis (MST, see Methods). AtHFR1 bound the COP1 WD40 domain with a dissociation constant (K_D) of $\sim 120 \mu\text{M}$ (Figs 5B and EV5). The ChHFR1 VP peptide showed only weak binding to COP1 WD40, with a K_D in the millimolar range (Figs 5B and EV5). Importantly, a second putative VP sequence in At/ChHFR1 showed no detectable binding, while the previously characterized *A. thaliana* cryptochrome 1 (AtCRY1) and the human HsTRIB1 VP sequences bound COP1 WD40 with a K_D in the $\sim 1 \mu\text{M}$ range, in good agreement with earlier isothermal titration calorimetry binding assays (Figs 5B and EV5) (Lau *et al*, 2019). Taken together, AtHFR1 VP peptide interacted more strongly with COP1 WD40, suggesting that AtHFR1 may represent a better substrate for COP1 than ChHFR1.

Next, we aimed to explore if these differences in COP1 affinity had an impact in the subsequent degradation of AtHFR1 and ChHFR1 proteins. To test this possibility, we generated chimeric *HFR1* genes in which the VP region was swapped, named as *ChHFR1** and *AtHFR1** (Fig 5C). *ChHFR1** differed from *ChHFR1* in the VP region, that was substituted for the AtHFR1-VP1. Reciprocally, *AtHFR1** contained the ChHFR1-VP region. Like the wild-type versions, these *HFR1* derivative genes were fused to the 3xHA and placed under the control of the 35S promoter (Fig 5C). When transiently expressed in tobacco leaves, ChHFR1* was now less abundant than AtHFR1*, suggesting that the VP regions contain enough information to determine the pattern of stability of the resulting HFR1 protein (Fig 5D). Because AtHFR1-VP1 binds to COP1 WD40 domain with higher affinity than ChHFR1-VP1, these results indicate a negative correlation of the binding affinity to COP1 with the accumulation (i.e., the higher the affinity the lower the accumulation). Hence, we concluded that in the HFR1 context, a stronger binding to COP1 results in lower abundance.

HFR1 interacts with PIF7

AtHFR1 has been shown to interact with all the members of the photolabile AtPIF quartet (PIF1, PIF3, PIF4, and PIF5). Using a yeast two-hybrid (Y2H) assay, we observed that AtHFR1 homodimerized, which indicated that its HLH domain is functional in this assay (Fig 6A). In the same assay, AtHFR1 was also shown to interact with AtPIF7 (Fig 6A). These results agree with recent data (Zhang *et al*, 2019). Because AtPIF7 is the main PIF in *A. thaliana*

promoting hypocotyl elongation in response to low R:FR (Li *et al*, 2012), we aimed to address whether HFR1 also interacts genetically with PIF7. First, we analyzed the genetic interaction between AtHFR1 and AtPIF7. After crossing *A. thaliana hfr1-5* with *pif7-1* and *pif7-2* mutants, we analyzed the hypocotyl response of the obtained double mutants in different low R:FR conditions. As expected, *hfr1* hypocotyls were longer and those of *pif7* mutants were shorter compared to *At*^{WT} under both W + FR conditions used (Fig 6B). In W and low R:FR (0.06), double *pif7 hfr1* mutant seedlings behaved mostly as *pif7* single mutants. However, under very low R:FR (0.02), they elongated similar to *At*^{WT} hypocotyls (Fig 6B). Together, these results indicate that *pif7* is epistatic over *hfr1* under low R:FR, whereas it seems additive under very low R:FR, two conditions that we speculate as mimicking proximity and canopy shade, respectively (Martinez-Garcia *et al*, 2014).

To further analyze the HFR1-PIF7 interaction, we aimed to test if *HFR1* overexpression will interfere with *PIF7* overexpression and impede its effects. For HFR1, we used a line overexpressing a stable but truncated form of the protein (missing the N-terminal, 35S:GFP- Δ Nt-HFR1, line #03) that strongly inhibits shade-induced hypocotyl elongation in *A. thaliana* without affecting other aspects of the seedling development (Galstyan *et al*, 2011) (Fig 6C and D). For PIF7, we used two available 35S:PIF7-CFP lines (#1 and #2) (Leivar *et al*, 2008) that were almost unresponsive to W + FR (Fig 6C) and smaller and less developed than the *At*^{WT} in W (Fig 6D). The inhibition of shade-induced elongation observed in the 35S:PIF7-CFP lines contrasts with the positive effect of growth observed by several other authors when overexpressing PIF7 fused to smaller tags (Flash-tag peptide) (Li *et al*, 2012), likely caused by toxic or squelching effects caused by high levels of the PIF7-CFP protein. In W, 35S:GFP- Δ Nt-HFR1 35S:PIF7-CFP double transgenic seedlings (#1 and #2) did not differ in hypocotyl length and general aspect with *At*^{WT}; interestingly, they did elongate clearly in low and very low R:FR (Fig 6C and D). The recovery of the shade-induced hypocotyl elongation and size of the seedlings took place even though *HFR1* transcript levels were significantly lower than in the 35S:GFP- Δ Nt-HFR1 parental line. *PIF7* transcript levels were not significantly different in the double transgenic seedlings than in their respective parental lines (Appendix Fig S2). Therefore, the inhibitory effect of *PIF7*-CFP overexpression appeared to be counteracted by the overexpression of the truncated *HFR1*, further supporting the genetic interaction between HFR1 and PIF7 (Fig 6C and D).

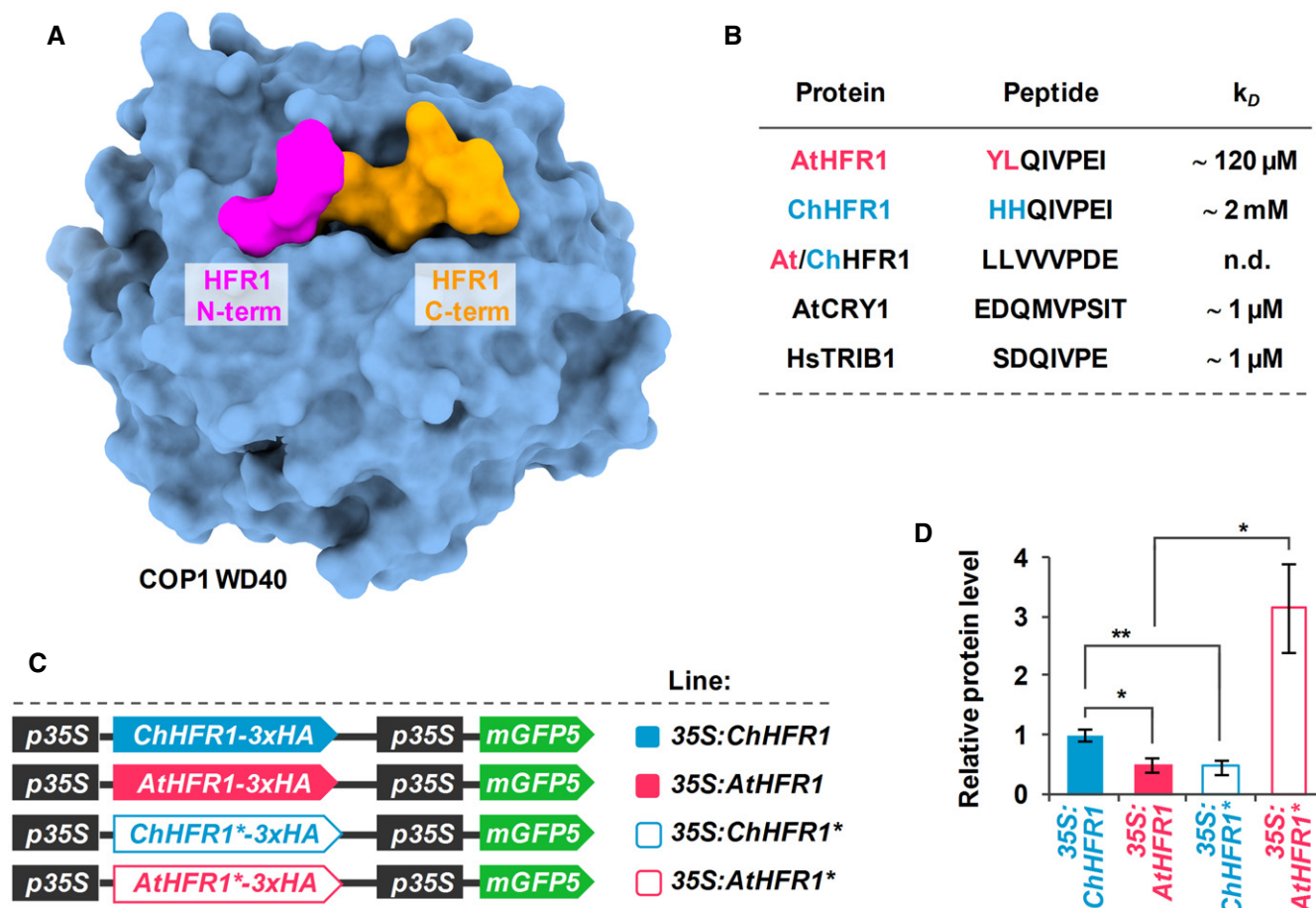


Figure 5. AtHFR1 interacts more strongly than ChHFR1 with the WD40 domain of COP1.

A Overview of the COP1 WD40-AtHFR1 complex (PDB ID 6QTV). The COP1 WD40 domain and the AtHFR1 VP peptide are shown in surface representation and colored in blue and orange, respectively. The N-terminus of HFR1 VP peptide, the amino acid of which differs between AtHFR1 and ChHFR1, is highlighted in magenta.

B Table summaries of the microscale thermophoresis binding assay (see Fig EV5). The sequence of the respective synthetic peptides is indicated.

C Cartoon of constructs containing *ChHFR1*, *AtHFR1*, *ChHFR1** and *AtHFR1** derivatives under the 35S promoter used for transient expression of transgenes in *N. benthamiana* leaves.

D Relative HFR1 protein levels, normalized to the GFP levels, are the means \pm SE of four independent biological replicates. Asterisks mark significant differences (Student's t-test: **P*-value < 0.05, ***P*-value < 0.01) between the indicated pairs.

Source data are available online for this figure.

Altogether, these analyses support that HFR1 and PIF7 interaction is important for the regulation of hypocotyl elongation in response to shade. These results are consistent with HFR1 functioning as a suppressor of PIF7.

HFR1 restrains PIF activity in *Cardamine hirsuta*

The similarity between shade-induced and warm temperature-induced hypocotyl elongation (thermomorphogenesis) suggests common underlying mechanisms. In *A. thaliana*, the increased activity of HFR1 at warm temperatures was previously shown to provide an important restraint on PIF4 action that drives elongation growth (Foreman *et al.*, 2011). Similarly, we hypothesized that the increased activity of HFR1 in *C. hirsuta* might restrain PIF activity more efficiently and consequently alter thermomorphogenesis

(Fig 7A). We analyzed this response by growing seedlings constantly at 22°C, 28°C, or transferred from 22°C to 28°C after day 2 (Fig 7B). Whereas warm temperature promoted hypocotyl elongation of *At*^{WT} seedlings compared to those growing at 22°C, *pif7* and *pif7-2* mutant seedlings were almost unresponsive to 28°C, in accordance with the role of PIF4, PIF5, and PIF7 in thermomorphogenesis (Stavang *et al.*, 2009; Franklin *et al.*, 2011; Fiorucci *et al.*, 2020). Unlike the *hfr1-5* mutant, which was slightly but significantly more responsive than *At*^{WT}, *A. thaliana* seedlings that overexpress a stable form of HFR1 (35S:GFP- Δ Nt-HFR1, Δ NtHFR1) were almost unresponsive to 28°C (Fig 7C), indicating that HFR1 activity impacts this PIF-dependent response. A lack of hypocotyl elongation was also observed in *Ch*^{WT} at 28°C, a response that was recovered in the *C. hirsuta chfr1* mutant seedlings (Fig 7C). These results support our hypothesis that a strong suppression of PIFs by the enhanced

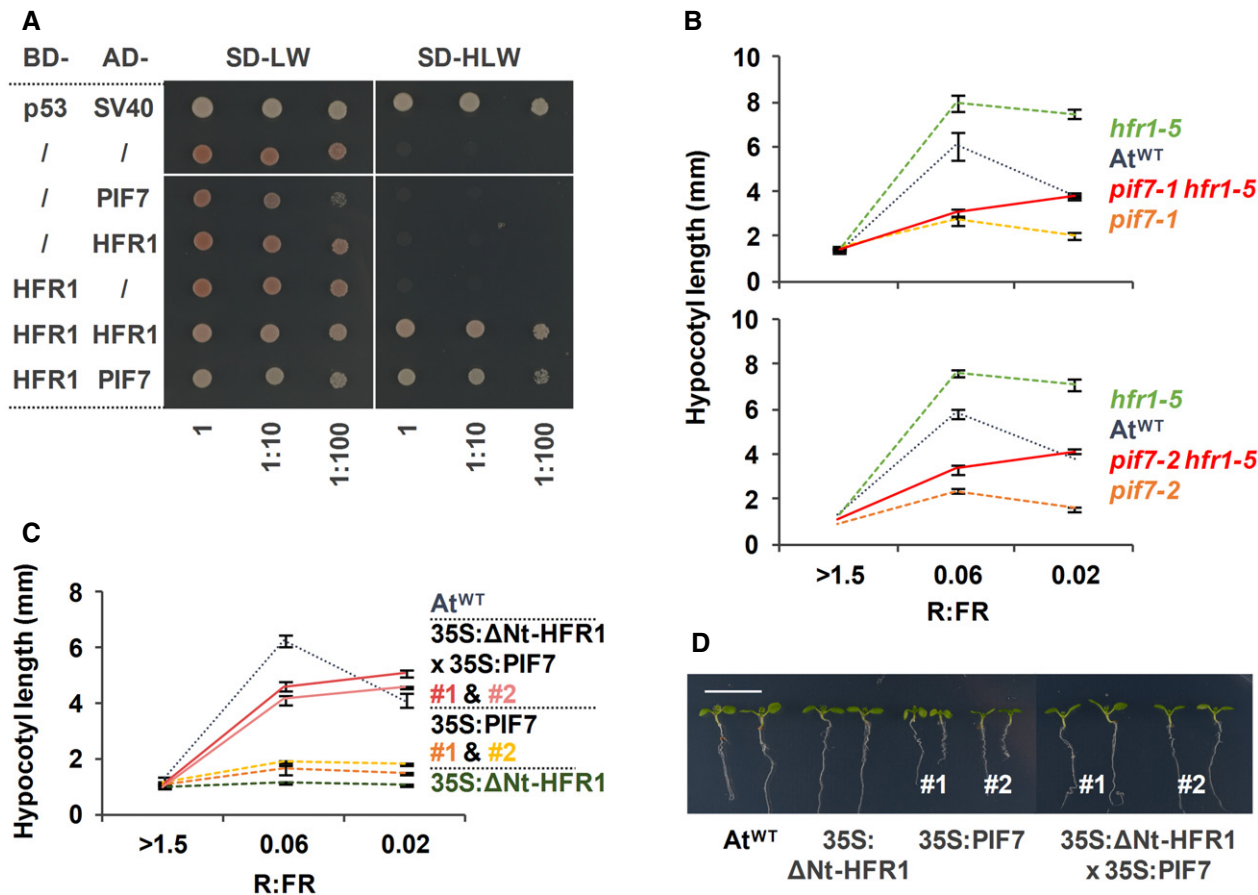


Figure 6. AtHFR1 interacts with AtPIF7.

- A** Y2H growth assay showing the interaction between AtHFR1 and AtPIF7. The BD- and the AD-derivative constructs used in the assay are shown on the left side of the panel. SD-LW or SD-HLW refer to the selective medium (plated as drops in dilutions of 1, 1:10, and 1:100) indicative of transformed cells or interaction between the hybrid proteins, respectively. Truncated forms of murine p53 (BD-fused) and SV40 large T-antigen (AD-fused), known to interact, were used as a positive control. Empty vectors (/) were used as negative controls.
- B, C** Hypocotyl length of seedlings of At^{WT}, (B) *pif7-1*, *hfr1-5*, *pif7-1 hfr1-5* (top graph), *pif7-2*, *hfr1-5*, and *pif7-2 hfr1-5* (bottom graph) mutants, and (C) transgenic 35S:GFP-ΔNt-HFR1 (35S:ΔNt-HFR1), two lines of 35S:PIF7-CFP (35S:PIF7 #1 and #2), and 35S:GFP-ΔNt-HFR1 35S:PIF7-CFP double transgenic (35S:ΔNt-HFR1 × 35S:PIF7 #1 and #2) seedlings grown under different R:FR. Seedlings were grown in W (R:FR > 1.5) for 7 days or for 2 days in W and then transferred to two W + FR treatments (R:FR 0.06 or 0.02) for 5 additional days. Values of hypocotyl length are the means ± SE of three independent biological replicates (at least 10 seedlings per replica).
- D** Aspect of representative 7-day-old W-grown seedlings shown in C. Scale bar is 1 cm.

HFR1 activity is responsible for the lack of hypocotyl elongation at 28°C of Ch^{WT} seedlings (Fig 7A). Together, our results suggest that the activity of the PIF-HFR1 regulatory module might be a general mechanism to coordinate the hypocotyl elongation in response to both W + FR exposure and 28°C.

We also studied dark-induced senescence (DIS), another PIF-dependent process (Fig 7D). In *A. thaliana*, DIS can be induced by transferring light-grown seedlings to complete darkness, a process in which PIF4 and PIF5 have major roles (Sakuraba *et al*, 2014; Song *et al*, 2014; Liebsch & Keech, 2016). DIS results in a degradation of chlorophylls, which can be quantified as markers of senescence progression (Sakuraba *et al*, 2014; Song *et al*, 2014). To examine DIS, we transferred light-grown At^{WT}, *pifq*, and Ch^{WT} seedlings to total darkness for up to 20 days (Fig 7E). After DIS was activated, At^{WT} seedlings became pale and eventually died. After just 5 days

of darkness, chlorophyll levels dropped, and longer dark treatments resulted in pronounced differences between the three genotypes. At^{WT} seedlings became visibly yellow at day 10, accompanied by a strong reduction of chlorophyll levels that dropped to less than 10% (Fig 7F). DIS was delayed in 35S:GFP-ΔNt-HFR1 seedlings, supporting that a stable HFR1 form can interfere with PIF activity in regulating this trait. However, DIS in was not advanced in *hfr1* mutants (Fig 7E). In Ch^{WT} seedlings, chlorophyll levels declined more slowly and seedlings were still green after 20 days of darkness, just like *pifq* (Fig 7E). The observed delay in the DIS in *C. hirsuta* was not affected in *chfr1* mutants, suggesting that HFR1 does not regulate this trait in any of the two species. It also pointed to a reduced PIF activity as the main cause for the delayed DIS in this species (Fig 7D–F). As HFR1 is very unstable, particularly in dark-grown conditions (Duek *et al*, 2004; Yang *et al*, 2005), it seems plausible

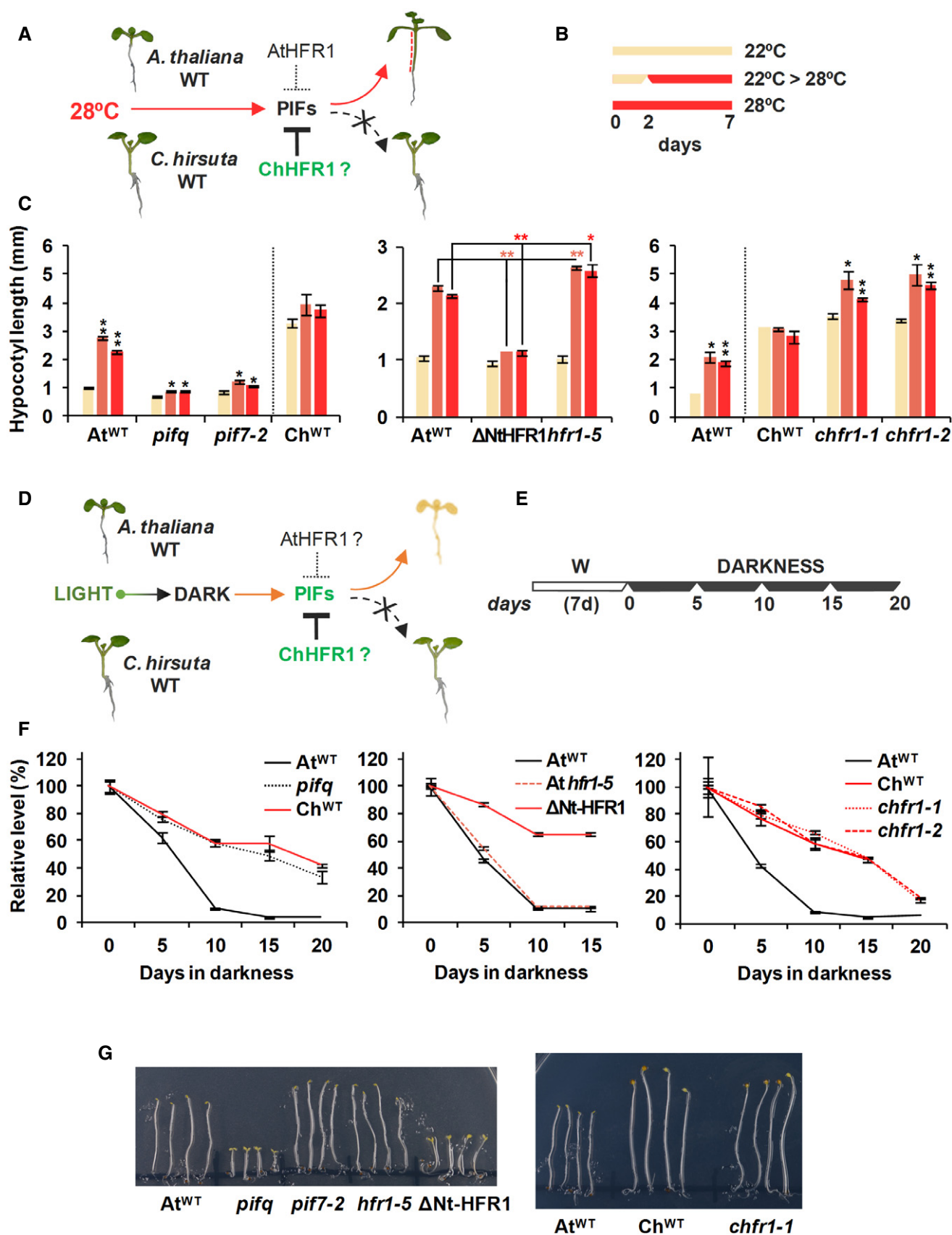


Figure 7.

Figure 7. *Cardamine hirsuta* has an attenuated hypocotyl elongation at warm temperature and delayed dark-induced senescence (DIS).

- A In At^{WT} , PIFs promote hypocotyl elongation as a response to warm temperature (28°C). High ChHFR1 activity is expected to inhibit this response by repressing PIFs more effectively in Ch^{WT} and attenuate hypocotyl elongation at 28°C.
- B Seedlings were grown for 7 days in W at either 22°C, 2 days at 22°C then transferred to 28°C for additional 5 days (22°C > 28°C) or for 7 days at 28°C, as represented in the panel.
- C Hypocotyl length of seedlings of (left) At^{WT} , *pifq*, *pif7-2*, Ch^{WT} , (middle) 35S::GFP-ΔNt-HFR1 (ΔNtHFR1), *hfr1-5* and (right) *chfr1-1* and *chfr1-2* lines grown at warm temperatures. Hypocotyl lengths are the means ± SE of three biological replicates. Asterisks mark significant differences (Student's *t*-test: **P*-value < 0.05, ***P*-value < 0.01) relative to the same genotype grown at 22°C (left and right graphs, black asterisks), and between the indicated pairs (middle graph, red asterisks).
- D In At^{WT} , PIF-mediated DIS involves a reduction of chlorophyll levels. HFR1 activity might inhibit DIS through repression of PIFs. If PIF activity is attenuated in Ch^{WT} , DIS would be delayed in this species compared to At^{WT} .
- E Seedlings were grown for 7 days in W and then transferred to total darkness for several days to induce senescence, as illustrated at the right panel.
- F Relative chlorophyll levels of (left) At^{WT} , *pifq*, Ch^{WT} , (middle) ΔNtHFR1, *hfr1-5* and (right) *chfr1-1*, and *chfr1-2* lines after DIS was promoted for the indicated time. For each genotype, values are relative to pigment levels at time 0 (7 days in W). Data are the means ± SE of four independent biological replicates.
- G Aspect of 4-day-old dark-grown seedlings of At^{WT} , *pifq*, *pif7-2*, *hfr1-5* and ΔNt-HFR1 (left panel), and At^{WT} , Ch^{WT} , and *chfr1-1* (right panel).

that HFR1 does not accumulate in seedlings when transferred to the dark. Despite this attenuation of PIF activity, Ch^{WT} seedlings showed an etiolated phenotype similar to that of At^{WT} when grown in the dark, in contrast to *A. thaliana pifq* and 35S::GFP-ΔNt-HFR1 seedlings (Fig 7G), suggesting the PIF activity is high enough in *C. hirsuta* to induce the normal skotomorphogenic development.

Discussion

It is currently unknown whether the switch between shade avoidance and tolerance strategies is an easily adjustable trait in plants. The existence of closely related species with divergent strategies to acclimate to shade provides a good opportunity to study the genetic and molecular basis for adapting to this environmental cue. To this goal, we performed comparative analyses of the hypocotyl response to shade in young seedlings of two related Brassicaceae: *A. thaliana* and *C. hirsuta*. *Arabidopsis thaliana*, a model broadly used to study the SAS hypocotyl response, is well characterized on a physiological, genetic, and molecular level. *Cardamine hirsuta* was previously described as a shade-tolerant species whose hypocotyls are unresponsive to simulated shade (Hay *et al*, 2014; Molina-Contreras *et al*, 2019). Recent work showed that phyA is a major contributor to the suppression of hypocotyl elongation of *C. hirsuta* seedlings in response to shade, mainly due to the stronger phyA activity in this species compared to the shade-avoider *A. thaliana* (Molina-Contreras *et al*, 2019). Importantly, an enhanced phyA activity was not enough to explain the lack of shade-induced hypocotyl elongation in *C. hirsuta*, pointing to additional components that contribute to this response. Our aim to fill this gap led us to uncover a role for HFR1 in this response.

In *C. hirsuta*, removal of HFR1 function resulted in a strong *slender in shade* (*sis*) phenotype but milder than that of *sis1* plants, deficient in the phyA photoreceptor (Molina-Contreras *et al*, 2019), providing genetic evidence for the role of HFR1 in restraining the *C. hirsuta* hypocotyl elongation in shade (Fig 1A and B). This indicates that, like phyA, HFR1 contributes to implement the shade-tolerant habit in *C. hirsuta* seedlings. Because of the *sis* phenotype of *chfr1* and RNAi-HFR1 seedlings (Fig 1), we hypothesized that HFR1 activity is higher in *C. hirsuta* than in *A. thaliana*. Consistently, transcript levels of HFR1 were significantly higher in Ch^{WT} than At^{WT} seedlings in both W and W + FR (Fig 2). Higher HFR1 levels in *C. hirsuta* may not be relevant in W because of the

expected lower abundance and activity of PIFs, but a higher pool of ChHFR1 ready to suppress early ChPIF action in shade could provide a fast and sustained repression of the elongation response. Indeed, the shade-induced expression of *PIL1*, *YUC8*, and *XTR7*, known to be direct PIF target genes in *A. thaliana*, was strongly and rapidly enhanced in *chfr1* and RNAi-HFR1 seedlings (Fig 1C and D). More importantly, rapid shade-induced expression was globally attenuated in Ch^{WT} compared to At^{WT} seedlings (Molina-Contreras *et al*, 2019).

In addition to changes in gene expression, a higher HFR1 activity in *C. hirsuta* could also result from post-translational regulation affecting protein stability. Our immunoblot analyses indicated that HFR1 proteins rapidly accumulate in response to simulated shade (W + FR), likely as a consequence of the strong shade-induced responsiveness of the promoter (Fig 4A). These results support that regulation of HFR1 protein abundance in low R:FR occurs mainly at the transcriptional level, as suggested (de Wit *et al*, 2016). More importantly, ChHFR1 accumulates significantly more when expressed under the control of a constitutive promoter either under W or W + FR (Fig 4B–D) suggesting that intrinsic differences in post-translational stability between these proteins play a role in their contrasting accumulation.

AtHFR1 protein abundance is modified post-translationally by phosphorylation (Park *et al*, 2008) and ubiquitination in a light- and COP1-dependent manner (Jang *et al*, 2005; Yang *et al*, 2005). Canopy shade promotes nuclear accumulation of COP1 (Pacin *et al*, 2013; Pacin *et al*, 2016) allowing it to directly interact with and polyubiquitinate AtHFR1, leading to its degradation by the 26S proteasome (Jang *et al*, 2005; Yang *et al*, 2005; Huang *et al*, 2014). AtHFR1, like ChHFR1, contains two putative COP1 binding sites (VP motifs) on its N-terminal half (Fig EV4A), although only one binds COP1 (Figs 5A and EV5) (Lau *et al*, 2019). Deletion of AtHFR1 Nt leads to its stabilization in the dark and light (Duek *et al*, 2004) and results in a stronger biological activity (Jang *et al*, 2005; Yang *et al*, 2005; Galstyan *et al*, 2011), highlighting the importance of the COP1-interacting domain for light regulation of AtHFR1 stability. Our MST binding assays showed that AtHFR1 binds to COP1 about 100 times more weakly than other plant COP1 substrates do (Lau *et al*, 2019), and ChHFR1 even more weakly than AtHFR1 (Fig 5A and B). AtHFR1 and ChHFR1 primary structures are similar, including the putative COP1-interacting domain (Jang *et al*, 2005), except for the addition of 30 amino acids at the N-terminal part of ChHFR1 and a 9-amino acid insertion in the C-terminal part of AtHFR1

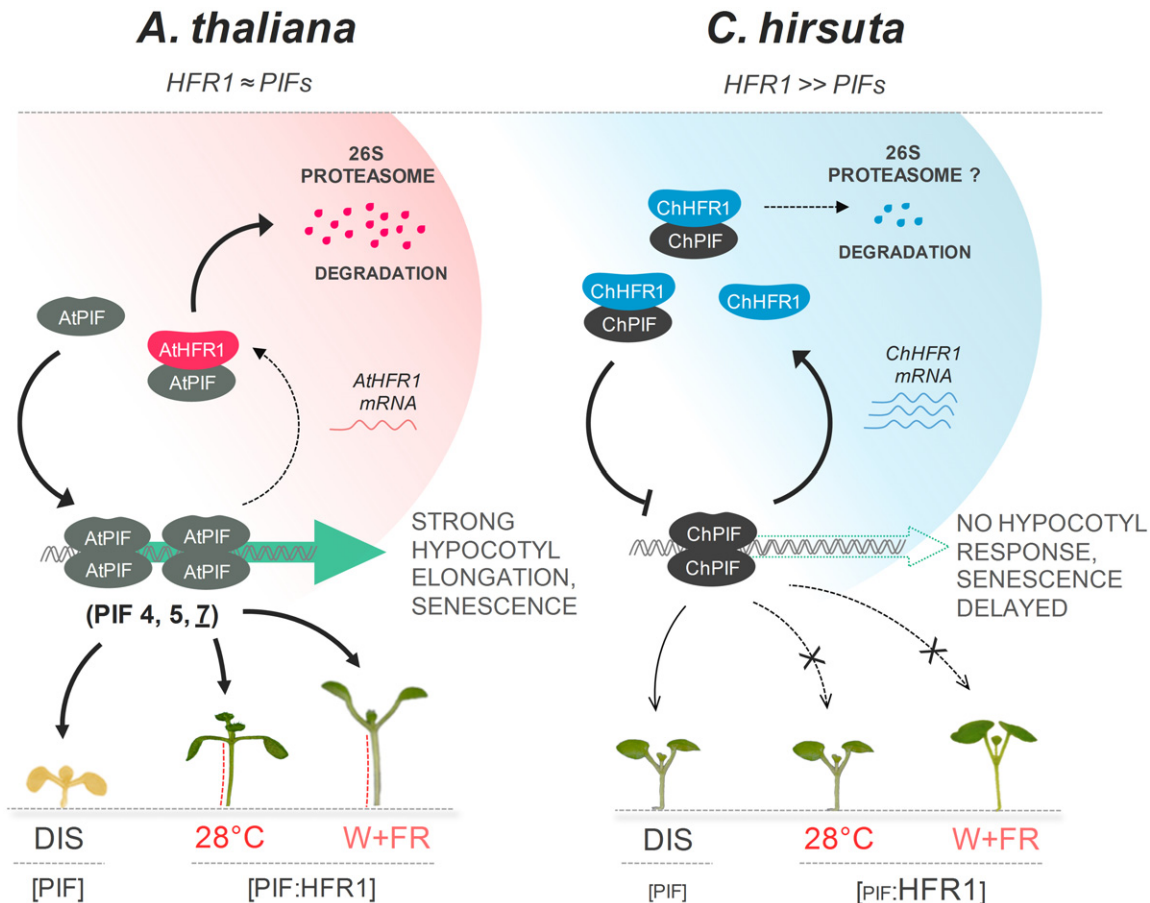


Figure 8. Model summarizing how PIF-HFR1 transcriptional module is differently balanced in *Arabidopsis thaliana* and *Cardamine hirsuta*.

Shade (low R:FR) displaces phytochrome photoequilibrium toward the inactive form, allowing PIFs to promote the expression of shade avoidance-related genes, such as *HFR1*. PIF transcript or/and protein levels are induced in response to warm temperatures, resulting in enhanced expression of growth-promoting genes. HFR1 abundance is also increased by warm temperature. HFR1 modulates these responses by heterodimerizing with PIFs and inhibiting their DNA-binding ability. As a result, HFR1 attenuates hypocotyl elongation of *A. thaliana* seedlings in response to shade or warm temperature. In *C. hirsuta*, higher HFR1 activity inhibits more effectively PIF action than in *A. thaliana*. In addition, PIF abundance is attenuated in *C. hirsuta*. Both changes alter the PIF-HFR1 balance in *C. hirsuta*, resulting in lower PIF transcriptional activity. As a consequence, shade- and warm temperature-induced hypocotyl elongation are repressed and DIS is delayed in this species.

(Fig EV4A). We cannot discount the possibility that protein sequence and/or structural differences other than the VP motifs could also contribute to the affinity of the full-length HFR1 orthologues for COP1 and account for the difference in abundance between *C. hirsuta* and *A. thaliana* HFR1. However, the strong impact of swapping the VP region between ChHFR1 and AtHFR1 on the abundance of the resulting HFR1* proteins (Fig 5C and D) further points to the binding affinity of COP1 for its substrates as a main determinant of the stability of the two HFR1 orthologues. Together, our results point to (i) the regulation of affinity for COP1 as impacting HFR1 stability and (ii) HFR1 stability as a mechanism to control global HFR1 activity to modulate adaptation of different plant species to vegetation proximity and shade.

AtHFR1 was previously shown to interact with all the AtPIFQ members and to form non-DNA-binding heterodimers (Fairchild *et al.*, 2000; Hornitschek *et al.*, 2012; Shi *et al.*, 2013). Our genetic and Y2H experiments extended the list of AtHFR1 interactors to AtPIF7, the major SAS-promoting PIF (Fig 6). If ChHFR1 maintains

similar PIF-binding abilities, the reduced expression of *ChPIF7* (Fig 2) might further contribute to imbalance the PIF-HFR1 module in favor of the negative HFR1 activity in *C. hirsuta* compared to *A. thaliana*. Because of the higher stability of ChHFR1 over AtHFR1 in shade (Fig 4), an even stronger repression of global PIF activity in *C. hirsuta* would contribute to the unresponsiveness of hypocotyls to shade. The attenuation of the warm temperature-induced hypocotyl elongation in *C. hirsuta*, which is a PIF-regulated process in *A. thaliana* (Koini *et al.*, 2009; Stavang *et al.*, 2009; Hayes *et al.*, 2017; Fiorucci *et al.*, 2020) and HFR1-dependent in both species (Fig 7A–C), further agrees with our proposal of an enhanced activity of HFR1 in *C. hirsuta* compared to *A. thaliana*. On the other hand, the delayed DIS observed in *C. hirsuta*, shown to be PIF-regulated in *A. thaliana* (Sakuraba *et al.*, 2014; Song *et al.*, 2014) but unaffected by HFR1 in the two species analyzed (Fig 7D and E), suggests that PIF activity is globally lower *per se* in *C. hirsuta* than in *A. thaliana*. Together, our results indicate that PIF-HFR1 module is balanced differently in *C. hirsuta* by the

combination of (i) an attenuated global PIF activity and *PIF7* expression compared to *A. thaliana* and (ii) the increased levels of ChHFR1 in light and shade conditions, resulting in the repression of PIF-regulated processes in *C. hirsuta* (Fig 8). Importantly, although attenuated, PIF activity in *C. hirsuta* is enough to provide a functional and effective etiolation response (Fig 7G) for seedlings survival during germination in the dark.

Activity of HFR1 and phyA (Molina-Contreras *et al*, 2019) appears to be increased in *C. hirsuta* to maintain unresponsiveness of hypocotyls to shade. An aspect shared by both negative regulators is that their expression and/or stability are strongly affected by light conditions. Expression of both *PHYA* and *HFR1* is induced by simulated shade in de-etiolated seedlings. By contrast, whereas the stability of the photolabile phyA is reduced by light but enhanced by shade, that of AtHFR1 is promoted by light and decreased by shade (Kircher *et al*, 1999; Duek *et al*, 2004; Park *et al*, 2008; Ciolfi *et al*, 2013; Casal *et al*, 2014; Martinez-Garcia *et al*, 2014; Pacin *et al*, 2016; Yang *et al*, 2018). Although expression of both *PHYA* and *HFR1* is higher in *C. hirsuta* than in *A. thaliana*, different mechanisms might contribute to their increased activity in *C. hirsuta*. Indeed, enhanced ChphyA repression was achieved by its stronger specific intrinsic activity (Molina-Contreras *et al*, 2019). By contrast, enhanced ChHFR1 repression was accomplished through its higher gene expression and protein stability coupled with an attenuated PIF7 activity. Altogether this could provide a more repressive state of the *C. hirsuta* PIF-HFR1 module. Because of the temporal differences downregulating many of the shade marker genes between phyA (observed after 4–8 h of shade exposure) (Molina-Contreras *et al*, 2019) and HFR1 (rapidly detected after just 1 h of shade exposure) (Fig 1C and D), it seems likely that ChHFR1 and ChphyA suppressor mechanisms of shade response in *C. hirsuta* act independently, as it was reported for *A. thaliana* (Ciolfi *et al*, 2013; Ortiz-Alcaide *et al*, 2019). Therefore, the concerted activity of these two independent suppressor mechanisms seems to coordinately prevent the shade-induced hypocotyl elongation in *C. hirsuta*. Whether other shade-tolerant species employ the same adaptive principles is something we aim to explore in the future.

Materials and Methods

Plant material and growth conditions

Arabidopsis thaliana *hfr1-5*, *pif7-1*, *pif7-2*, and *pifq* mutants, 35S:PIF7-CFP and 35S:GFP-ΔNt-HFR1 lines (in the Col-0 background, At^{WT}) and *Cardamine hirsuta* (Oxford ecotype, Ox, Ch^{WT}) plants have been described before (Yang *et al*, 2005; Leivar *et al*, 2008; Galstyan *et al*, 2011; Hay *et al*, 2014). Plants were grown in the greenhouse under long-day photoperiods (16 h light and 8 h dark) to produce seeds, as described (Martinez-Garcia *et al*, 2014; Gallemi *et al*, 2016; Gallemi *et al*, 2017). For transient expression assays, *Nicotiana benthamiana* plants were grown in the greenhouse under long-day photoperiods (16 h light and 8 h dark).

For hypocotyl assays, seeds were surface-sterilized and sown on solid growth medium without sucrose (0.5×GM–). For gene

expression analyses, immunoblot experiments and pigment quantification, seeds were sown on a sterilized nylon membrane placed on top of the solid 0.5×GM– medium. After stratification (dark at 4°C) of 3–6 days, plates with seeds were incubated in plant chambers at 22°C under continuous white light (W) for at least 2 h to break dormancy and synchronize germination (Paulisic *et al*, 2017; Roig-Villanova *et al*, 2019).

W was emitted from cool fluorescent tubes that provided from 20 to 100 μmol/m²·s¹ of photosynthetically active radiation (PAR) with a red (R) to far-red light (FR) ratio (R:FR) from 1.3 to 3.3. The different simulated shade treatments were produced by supplementing W with increasing amounts of FR (W + FR). FR was emitted from GreenPower LED module HF far-red (Philips), providing R:FR of 0.02–0.09. Light fluence rates were measured with a Spectrosense2 meter (Skye Instruments Ltd), which measures PAR (400–700 nm), and 10 nm windows of R (664–674 nm) and FR (725–735 nm) regions (Martinez-Garcia *et al*, 2014). Details of the resulting light spectra have been described before (Molina-Contreras *et al*, 2019).

Temperature-induced hypocotyl elongation assays were done by placing the plates with seeds under the indicated light conditions in growth chambers at 22°C or 28°C.

Measurement of hypocotyl length

Hypocotyl length was measured as described (Paulisic *et al*, 2017; Roig-Villanova *et al*, 2019). Experiments were repeated at least three times with more than 10 seedlings per genotype and/or treatment, providing consistent results. Hypocotyl measurements from the different experiments were averaged.

Generation of transgenic lines, mutants, and crosses

Arabidopsis thaliana *hfr1-5* plants were transformed to express AtHFR1 and ChHFR1 under the promoters of 35S or AtHFR1 (pAt). The obtained lines were named as *hfr1>35S:ChHFR1*, *hfr1>pAt:AtHFR1*, and *hfr1>pAt:ChHFR1*. Transgenic RNAi-HFR1 and mutant *chfr1-1* and *chfr1-2* lines are in Ch^{WT} background. Details of the constructs used for the generation of these lines (Morineau *et al*, 2017) are provided as Appendix Supplementary Methods.

Gene expression analyses

Real-time qPCR analyses were performed using biological triplicates, as indicated (Gallemi *et al*, 2017). Total RNA was extracted from seedlings, treated as indicated, using commercial kits (Maxwell[®] SimplyRNA and Maxwell[®] RSC Plant RNA Kits; www.promega.com). 2 μg of RNA was reverse-transcribed with Transcriptor First Strand cDNA synthesis Kit (Roche, www.roche.com). The *A. thaliana* *UBIQUITIN 10* (*UBQ10*) was used for normalization in *A. thaliana* *hfr1-5* lines expressing AtHFR1 or ChHFR1. The *ELONGATION FACTOR 1α* (*EF1α*), *YELLOW-LEAF-SPECIFIC GENE 8* (*YLS8*) and *SPC25* (AT2G39960) were used for normalizing and comparing the levels of HFR1 and PIF7 between *A. thaliana* and *C. hirsuta* (Molina-Contreras *et al*, 2019). Primers sequences for qPCR analyses are provided in Appendix Table S1.

Expression of HFR1 derivatives in *Nicotiana benthamiana*

Nicotiana benthamiana plants were agroinfiltrated with *Agrobacterium tumefaciens* strains transformed with the plasmids to express the various HFR1 derivatives and kept in the greenhouse under long-day photoperiods. Samples (leaf circles obtained from infiltrated areas) were taken 3 days after agroinfiltration and frozen immediately. In Fig 4D, prior freezing, leaf circles were incubated in Petri dishes with 10 ml of the \pm CHX solution for the indicated times and conditions. Each biological sample contained about 75 mg of leaf tissue from the same leaf. Additional details of the preparation of the plasmids used are provided in Appendix Supplementary Methods.

Protein extraction and immunoblotting analyses

To detect and quantify transgenic AtHFR1 and ChHFR1, proteins were extracted from ~50 mg of 7-day-old seedlings (grown as indicated) or from 50 to 75 mg of agroinfiltrated *N. benthamiana* leaves. Plant material was frozen in liquid nitrogen, ground to powder and total proteins were extracted using an SDS-containing extraction buffer (1.5 μ l per mg of fresh weight), as described (Gallemi *et al.*, 2017). Protein concentration was estimated using Pierce™ BCA Protein Assay Kit (Thermo Scientific, www.thermo.com). Proteins (45–50 μ g per lane) were resolved on a 10% SDS-PAGE gel, transferred to a PVDF membrane and immunoblotted with rat monoclonal anti-HA (High Affinity, clone 3F10, Roche; 1:2,000 dilution) or mouse monoclonal anti-GFP (monoclonal mix, clones 7.1 + 13.1, Roche; 1:2,000 dilution). Secondary antibodies used were horseradish peroxidase (HRP)-conjugated goat anti-rat (Polyclonal, A9037, Sigma, www.sigmaaldrich.com; 1:5,000 dilution) and HRP-conjugated sheep anti-mouse (Promega; 1:10,000 dilution). Development of blots was carried out in ChemiDoc™ Touch Imaging System (Bio-Rad, www.bio-rad.com) using ECL Prime Western Blotting Detection Reagent (GE Healthcare, RPN2236). Relative protein levels of three to four biological replicates were quantified using Image Lab™ Software.

Yeast 2 hybrid assays

For yeast 2 hybrid (Y2H) assays, we employed a cell mating system, as described (Gallemi *et al.*, 2017). The leucine (Leu) auxotroph YM4271a yeast strain was transformed with the AD-derived constructs and the tryptophan (Trp) auxotroph pJ694 α strain with the BD-derived constructs. Colonies were selected on synthetic defined medium (SD) lacking Leu (SD-L) or Trp (SD-W), grown in liquid medium and set to mate by mixing equal volumes of transformed cells. Dilutions of the mated cells were selected on SD-LW, and protein interactions were tested on SD-LW medium lacking histidine (SD-HLW). Details of the yeast constructs used are provided as Appendix Supplementary Methods.

Expression of AtCOP1 WD40 protein and purification

AtCOP1 WD40 (residues 349–675) was expressed in *Spodoptera frugiperda* Sf9 cells (Thermo Fisher) and purified as described

previously (Lau *et al.*, 2019). Details of the procedure are provided as Appendix Supplementary Methods.

Protein labeling and microscale thermophoresis

COP1 WD40 was labeled using Monolith Protein Labeling Kit RED-NHS 2nd Generation Amine Reactive kit (MO-L011; Nanotemper Technologies, Munich, Germany). After the TEV cleavage, COP1 WD40 was in buffer A containing 2 mM β -ME, which is incompatible with the labeling procedure. Therefore, prior to labeling, the buffer was exchanged using labeling buffer NHS provided in the kit. In the last step, the protein was purified from the free dye, in the assay buffer 20 mM Hepes pH 7.5, 150 mM NaCl, 2 mM TCEP and 0.05% [v/v] Tween-20 in 12–15 different fractions. The absorbance of each sample was measured at 280 and 650 nm. The Degree of Labeling (DOL) was calculated using the formula provided in the manual. Aliquots containing 2,000 to 8,000 nM concentration of proteins and DOL of > 0.5 were flash frozen for the use in the assay.

Peptide solutions were freshly prepared in the assay buffer at desired concentrations. For each independent replicate, 10 μ l of peptide solution was serially diluted 1:1 using assay buffer, in 16 PCR tubes. 10 μ l of solution was discarded from the 16th tube, thus each tube contained 10 μ l of peptide solution. Each dilution step was mixed with 10 μ l of 150 nM of COP1 WD40 and transferred into Monolith NT.115 Premium Capillaries (MO-K025). The samples were measured with the Monolith NT.115 instrument at a 25% LED Power and 20% MST power. The resulting thermophoresis data were analyzed with the MOAffinityAnalysis software (Nanotemper Technologies).

Data availability

This study includes no data deposited in external repositories.

Expanded View for this article is available online.

Acknowledgements

We are grateful to Peter Quail (PGEC, Albany, CA, USA) for providing 35S:PIF7-CFP seeds; and to Manuel Rodríguez-Concepción (CRAG) for comments on the manuscript. SP received predoctoral fellowships from the *Agència d'Ajuts Universitaris i de Recerca* (AGAUR—Generalitat de Catalunya, FI programme). WQ is a recipient of a predoctoral Chinese Scholarship Council (CSC) fellowship. CT received a Marie Curie IEF postdoctoral contract funded by the European Commission and a CRAG short-term fellowship. We also acknowledge the support of the MINECO for the “Centro de Excelencia Severo Ochoa 2016–2019” award SEV-2015-0533 and by the CERCA Programme/Generalitat de Catalunya. FN research at the IJPB benefits from the support of the LabEx Saclay Plant Sciences-SPS (ANR-10-LABX-0040-SPS). Our research is supported by grants from BBSRC (BB/H006974/1) and Max Planck Society (core grant) to MT, and from MINECO-FEDER (BIO2017-85316-R) and AGAUR (2017-SGR1211 and Xarba) to JFM-G. MH is an International Research Scholar by the Howard Hughes Medical Institute.

Author contributions

JFM-G conceived the original research plan, and directed and coordinated the study. SP, WQ, CT, BA, and FN designed and/or carried out experiments using

A. thaliana and *C. hirsuta*. MT and FN fundamentally contributed to design the constructs to obtain *C. hirsuta* transgenic and mutant lines. HAV and MH designed and performed MST experiments and their analyses. SP and JFM-G wrote the article with contributions and/or comments of all other authors.

Conflict of interest

The authors declare that they have no conflict of interest.

References

- Ballare CL, Pierik R (2017) The shade-avoidance syndrome: multiple signals and ecological consequences. *Plant Cell Environ* 40: 2530–2543
- Bou-Torrent J, Galstyan A, Gallemi M, Cifuentes-Esquivel N, Molina-Contreras MJ, Salla-Martret M, Jikumaru Y, Yamaguchi S, Kamiya Y, Martinez-Garcia JF (2014) Plant proximity perception dynamically modulates hormone levels and sensitivity in *Arabidopsis*. *J Exp Bot* 65: 2937–2947
- Casal JJ (2013) Photoreceptor signaling networks in plant responses to shade. *Annu Rev Plant Biol* 64: 403–427
- Casal JJ, Candia AN, Sellaro R (2014) Light perception and signalling by phytochrome A. *J Exp Bot* 65: 2835–2845
- Cifuentes-Esquivel N, Bou-Torrent J, Galstyan A, Gallemi M, Sessa G, Salla-Martret M, Roig-Villanova I, Ruberti I, Martinez-Garcia JF (2013) The bHLH proteins BEE and BIM positively modulate the shade avoidance syndrome in *Arabidopsis* seedlings. *Plant J* 75: 989–1002
- Ciolfi A, Sessa G, Sassi M, Possenti M, Salvucci S, Carabelli M, Morelli G, Ruberti I (2013) Dynamics of the shade-avoidance response in *Arabidopsis*. *Plant Physiol* 163: 331–353
- de Wit M, Keuskamp DH, Bongers FJ, Hornitschek P, Gommers CMM, Reinen E, Martinez-Ceron C, Fankhauser C, Pierik R (2016) Integration of phytochrome and cryptochrome signals determines plant growth during competition for light. *Curr Biol* 26: 3320–3326
- Duek PD, Elmer MV, van Oosten VR, Fankhauser C (2004) The degradation of HFR1, a putative bHLH class transcription factor involved in light signaling, is regulated by phosphorylation and requires COP1. *Curr Biol* 14: 2296–2301
- Fairchild CD, Schumaker MA, Quail PH (2000) HFR1 encodes an atypical bHLH protein that acts in phytochrome A signal transduction. *Genes Dev* 14: 2377–2391
- Fiorucci AS, Fankhauser C (2017) Plant strategies for enhancing access to sunlight. *Curr Biol* 27: R931–R940
- Fiorucci AS, Galvao VC, Ince YC, Boccaccini A, Goyal A, Allenbach Petrolati L, Trevisan M, Fankhauser C (2020) PHYTOCHROME INTERACTING FACTOR 7 is important for early responses to elevated temperature in *Arabidopsis* seedlings. *New Phytol* 226: 50–58
- Foreman J, Johansson H, Hornitschek P, Josse EM, Fankhauser C, Halliday KJ (2011) Light receptor action is critical for maintaining plant biomass at warm ambient temperatures. *Plant J* 65: 441–452
- Franklin KA, Lee SH, Patel D, Kumar SV, Spartz AK, Gu C, Ye S, Yu P, Breen G, Cohen JD et al (2011) Phytochrome-interacting factor 4 (PIF4) regulates auxin biosynthesis at high temperature. *Proc Natl Acad Sci USA* 108: 20231–20235
- Galstyan A, Cifuentes-Esquivel N, Bou-Torrent J, Martinez-Garcia JF (2011) The shade avoidance syndrome in *Arabidopsis*: a fundamental role for atypical basic helix-loop-helix proteins as transcriptional cofactors. *Plant J* 66: 258–267
- Gallemi M, Galstyan A, Paulisic S, Then C, Ferrandez-Ayela A, Lorenzo-Orts L, Roig-Villanova I, Wang X, Micol JL, Ponce MR et al (2016) DRACULA2 is a dynamic nucleoporin with a role in regulating the shade avoidance syndrome in *Arabidopsis*. *Development* 143: 1623–1631
- Gallemi M, Molina-Contreras MJ, Paulisic S, Salla-Martret M, Sorin C, Godoy M, Franco-Zorrilla JM, Solano R, Martinez-Garcia JF (2017) A non-DNA-binding activity for the ATHB4 transcription factor in the control of vegetation proximity. *New Phytol* 216: 798–813
- Gommers CM, Visser EJ, St Onge KR, Voesenek LA, Pierik R (2013) Shade tolerance: when growing tall is not an option. *Trends Plant Sci* 18: 65–71
- Gommers CM, Keuskamp DH, Buti S, van Veen H, Koevoets IT, Reinen E, Voesenek LA, Pierik R (2017) Molecular profiles of contrasting shade response strategies in wild plants: differential control of immunity and shoot elongation. *Plant Cell* 29: 331–344
- Hay AS, Pieper B, Cooke E, Mandakova T, Cartolano M, Tattersall AD, Ioio RD, McGowan SJ, Barkoulas M, Galinha C et al (2014) Cardamine hirsuta: a versatile genetic system for comparative studies. *Plant J* 78: 1–15
- Hayes S, Sharma A, Fraser DP, Trevisan M, Cragg-Barber CK, Tavridou E, Fankhauser C, Jenkins GI, Franklin KA (2017) UV-B perceived by the UVR8 photoreceptor inhibits plant thermomorphogenesis. *Curr Biol* 27: 120–127
- Hersch M, Lorrain S, de Wit M, Trevisan M, Ljung K, Bergmann S, Fankhauser C (2014) Light intensity modulates the regulatory network of the shade avoidance response in *Arabidopsis*. *Proc Natl Acad Sci USA* 111: 6515–6520
- Hornitschek P, Lorrain S, Zoete V, Michielin O, Fankhauser C (2009) Inhibition of the shade avoidance response by formation of non-DNA binding bHLH heterodimers. *EMBO J* 28: 3893–3902
- Hornitschek P, Kohnen MV, Lorrain S, Rougemont J, Ljung K, Lopez-Vidriero I, Franco-Zorrilla JM, Solano R, Trevisan M, Pradervand S et al (2012) Phytochrome interacting factors 4 and 5 control seedling growth in changing light conditions by directly controlling auxin signaling. *Plant J* 71: 699–711
- Huang X, Ouyang X, Deng XW (2014) Beyond repression of photomorphogenesis: role switching of COP/DET/FUS in light signaling. *Curr Opin Plant Biol* 21: 96–103
- Jang IC, Yang JY, Seo HS, Chua NH (2005) HFR1 is targeted by COP1 E3 ligase for post-translational proteolysis during phytochrome A signaling. *Genes Dev* 19: 593–602
- Kircher S, Kozma-Bognar L, Kim L, Adam E, Harter K, Schafer E, Nagy F (1999) Light quality-dependent nuclear import of the plant photoreceptors phytochrome A and B. *Plant Cell* 11: 1445–1456
- Koini MA, Alvey L, Allen T, Tilley CA, Harberd NP, Whitelam GC, Franklin KA (2009) High temperature-mediated adaptations in plant architecture require the bHLH transcription factor PIF4. *Curr Biol* 19: 408–413
- Lau K, Podolec R, Chappuis R, Ulm R, Hothorn M (2019) Plant photoreceptors and their signaling components compete for COP1 binding via VP peptide motifs. *EMBO J* 38: e102140
- Leivar P, Monte E, Al-Sady B, Carle C, Storer A, Alonso JM, Ecker JR, Quail PH (2008) The *Arabidopsis* phytochrome-interacting factor PIF7, together with PIF3 and PIF4, regulates responses to prolonged red light by modulating phyB levels. *Plant Cell* 20: 337–352
- Li L, Ljung K, Breton G, Schmitz RJ, Pruneda-Paz J, Cowing-Zitron C, Cole BJ, Ivans LJ, Pedmale UV, Jung HS et al (2012) Linking photoreceptor excitation to changes in plant architecture. *Genes Dev* 26: 785–790
- Liebsch D, Keesh O (2016) Dark-induced leaf senescence: new insights into a complex light-dependent regulatory pathway. *New Phytol* 212: 563–570
- Lorrain S, Allen T, Duek PD, Whitelam GC, Fankhauser C (2008) Phytochrome-mediated inhibition of shade avoidance involves degradation of growth-promoting bHLH transcription factors. *Plant J* 53: 312–323
- Martinez-Garcia JF, Huq E, Quail PH (2000) Direct targeting of light signals to a promoter element-bound transcription factor. *Science* 288: 859–863

- Martinez-Garcia JF, Galleffi M, Molina-Contreras MJ, Llorente B, Bevilacqua MR, Quail PH (2014) The shade avoidance syndrome in *Arabidopsis*: the antagonistic role of phytochrome a and B differentiates vegetation proximity and canopy shade. *PLoS One* 9: e109275
- Mazza CA, Ballare CL (2015) Photoreceptors UVR8 and phytochrome B cooperate to optimize plant growth and defense in patchy canopies. *New Phytol* 207: 4–9
- Molina-Contreras MJ, Paulišić S, Then C, Moreno-Romero J, Pastor-Andreu P, Morelli L, Roig-Villanova I, Jenkins H, Hallab A, Gan X et al (2019) Photoreceptor activity contributes to contrasting responses to shade in *Cardamine* and *Arabidopsis* seedlings. *Plant Cell* 31: 2649–2663
- Morineau C, Bellec Y, Tellier F, Gissot L, Kelemen Z, Nogue F, Faure JD (2017) Selective gene dosage by CRISPR-Cas9 genome editing in hexaploid *Camelina sativa*. *Plant Biotechnol J* 15: 729–739
- Ortiz-Alcaide M, Llamas E, Gomez-Cadenas A, Nagatani A, Martinez-Garcia JF, Rodriguez-Concepcion M (2019) Chloroplasts modulate elongation responses to canopy shade by retrograde pathways involving HY5 and abscisic acid. *Plant Cell* 31: 384–398
- Pacin M, Legris M, Casal JJ (2013) COP1 re-accumulates in the nucleus under shade. *Plant J* 75: 631–641
- Pacin M, Semmoloni M, Legris M, Finlayson SA, Casal JJ (2016) Convergence of CONSTITUTIVE PHOTOMORPHOGENESIS 1 and PHYTOCHROME INTERACTING FACTOR signalling during shade avoidance. *New Phytol* 211: 967–979
- Park HJ, Ding L, Dai M, Lin R, Wang H (2008) Multisite phosphorylation of *Arabidopsis* HFR1 by casein kinase II and a plausible role in regulating its degradation rate. *J Biol Chem* 283: 23264–23273
- Paulišić S, Molina-Contreras MJ, Roig-Villanova I, Martinez-Garcia JF (2017) Approaches to study light effects on brassinosteroid sensitivity. *Methods Mol Biol* 1564: 39–47
- Pierik R, Testerink C (2014) The art of being flexible: how to escape from shade, salt, and drought. *Plant Physiol* 166: 5–22
- Roig-Villanova I, Bou-Torrent J, Galstyan A, Carretero-Paulet L, Portoles S, Rodriguez-Concepcion M, Martinez-Garcia JF (2007) Interaction of shade avoidance and auxin responses: a role for two novel atypical bHLH proteins. *EMBO J* 26: 4756–4767
- Roig-Villanova I, Paulišić S, Martinez-Garcia JF (2019) Shade avoidance and neighbor detection. *Methods Mol Biol* 2026: 157–168
- Sakuraba Y, Jeong J, Kang MY, Kim J, Paek NC, Choi G (2014) Phytochrome-interacting transcription factors PIF4 and PIF5 induce leaf senescence in *Arabidopsis*. *Nat Commun* 5: 4636
- Sasidharan R, Pierik R (2010) Cell wall modification involving XTHs controls phytochrome-mediated petiole elongation in *Arabidopsis thaliana*. *Plant Signal Behav* 5: 1491–1492
- Sessa G, Carabelli M, Sassi M, Ciolfi A, Possenti M, Mitterpergher F, Becker J, Morelli G, Ruberti I (2005) A dynamic balance between gene activation and repression regulates the shade avoidance response in *Arabidopsis*. *Genes Dev* 19: 2811–2815
- Shi H, Zhong S, Mo X, Liu N, Nezames CD, Deng XW (2013) HFR1 sequesters PIF1 to govern the transcriptional network underlying light-initiated seed germination in *Arabidopsis*. *Plant Cell* 25: 3770–3784
- Smith H (1982) Light quality, photoperception, and plant strategy. *Ann Rev Plant Physiol* 33: 481–518
- Song Y, Yang C, Gao S, Zhang W, Li L, Kuai B (2014) Age-triggered and dark-induced leaf senescence require the bHLH transcription factors PIF3, 4, and 5. *Mol Plant* 7: 1776–1787
- Stavang JA, Gallego-Bartolome J, Gomez MD, Yoshida S, Asami T, Olsen JE, Garcia-Martinez JL, Alabadi D, Blazquez MA (2009) Hormonal regulation of temperature-induced growth in *Arabidopsis*. *Plant J* 60: 589–601
- Valladares F, Niinemets U (2008) Shade tolerance, a key plant feature of complex nature and consequences. *Ann Rev Ecol Evol Syst* 39: 237–257
- van Gelderen K, Kang C, Paalman R, Keuskamp D, Hayes S, Pierik R (2018) Far-red light detection in the shoot regulates lateral root development through the HY5 transcription factor. *Plant Cell* 30: 101–116
- Yang J, Lin R, Sullivan J, Hoecker U, Liu B, Xu L, Deng XW, Wang H (2005) Light regulates COP1-mediated degradation of HFR1, a transcription factor essential for light signaling in *Arabidopsis*. *Plant Cell* 17: 804–821
- Yang C, Li L (2017) Hormonal regulation in shade avoidance. *Front Plant Sci* 8: 1527
- Yang C, Xie F, Jiang Y, Li Z, Huang X, Li L (2018) Phytochrome A negatively regulates the shade avoidance response by increasing auxin/indole acetic acid protein stability. *Dev Cell* 44: 29–41.e4
- Zhang R, Yang C, Jiang Y, Li L (2019) A PIF7-CONSTANS-Centered molecular regulatory network underlying shade-accelerated flowering. *Mol Plant* 12: 1587–1597